Detection of nematodes in soybean crop by drone[1]

Bruno Henrique Tondato Arantes[2], Victor Hugo Moraes[3], Alaerson Maia Geraldine[4], Tavvs Micael Alves[4], Alice Maria Albert[4], Gabriel Jesus da Silva[4], Gustavo Castoldi[4]

ABSTRACT - Global consumption of oilseeds has been growing progressively in the last five growing seasons, in which soybean represents 60% of this sector. Thus, in order to maintain a high production in the region of Rio Verde, State of Goiás, against the phytopathological problems, this study aimed to define the best spectral range for the detection of *H. glycines* and *P. brachyurus* by linear regressions in soybean at R3 stage, as well as the elaboration of mathematical models through multiple linear regressions. For this, soil and root were sampled in the experimental area, as well as a flight was performed with the Sentera sensor. Data were used for the elaboration of regressions and for the validation of 2 mathematical models. Significant values were observed in simple linear regression only for cysts, in the visible range, with a good R^2 value for the Green, Red and 568 nm bands, to nonviable cysts. When working with the stepwise statistics, better results are found for *H. glycines*, which now has an R^2(aj) of 0.7430 and *P. brachyurus* is then detected. From the mathematical model obtained with the multiple linear regression for non-viable cysts with an R^2(aj) of 0.7430, it is possible to detect the spatial distribution of nematodes across the soybean field, in order to perform a localized management, optimizing the applications. Good results are also possible using the mathematical model obtained by simple linear regression.

Key words: Remote sensing. Image processing. *Heterodera glycines. Pratylenchus brachyurus.* Digital Farmin*g*.

[2]Department of Agricultural Engineering, Universidade Federal do Rio Grande do Sul, Porto Alegre-RS, Brasil, bhtondato@gmail.com (ORCID ID 0000-0001-6339-5052)
[3]Universidade Federal de Goiás, Goiânia-GO, Brasil, victor.cm1@hotmail.com (0000-0002-6796-6139)
[4]Instituto Federal Goiano, Rio Verde - GO, Brasil, alaerson.geraldine@ifgoiano.edu.br (0000-0001-6794-9665), Tavvs.Alves@ifgoiano.edu.br (0000-0002-4660-9191), aliceberft@hotmail.com (0000-0002-3453-9333), gabrielljesus789@gmail.com, gustavo.castoldi@ifgoiano.edu.br (0000-0002-22062830)

INTRODUCTION

Global consumption of oilseeds has been growing steadily since the last five growing seasons, in which soybean represents 60% of this sector (UNITED STATES DEPARTMENT OF AGRICULTURE, 2019). However, just like any other crop, soybean suffers from reduced productivity due to plant pathogens. Among them, the two main ones are, *Heterodera glycines,* known as soybean cyst nematode, and *Pratylenchus brachyurus,* the root lesion nematode.

H. glycines is a pathogen that can survive in the soil for many years even without the presence of a host. It is possible because of the dormant stage called cyst, which is a means of survival, under unsuitable conditions for juveniles (MASONBRINK *et al.*, 2019). Symptoms are similar to nutrient and water shortage, which impairs plant development. As a consequence, soybean may exhibit stunted growth, chlorosis, reduced productivity, and even death due to the number of nematodes (BAJWA *et al.*, 2017; NIBLACK, 2005; SONG *et al.*, 2017; ZHANG *et al.*, 2017).

P. brachyurus, a migratory endoparasitic nematode (HOMIAK *et al.*, 2017), causes darkening of the main root system, reduced plant size, reduced grain number and size, and chlorosis in the canopy of the plant, which are similar to the symptoms induced by *H. glycines* (SANTANA-GOMES *et al.*, 2014). In order to avoid large yield losses, farmers have used non-host crop rotation, nematode-resistant cultivars and chemical and biological nematicides (DUTTA *et al.*, 2019). However, the application of nematicides throughout the area has a very high cost, which somehow encourages the search for alternative measures for the spot mapping of the occurrence of patches.

Precision agriculture is a suitable tool for mapping nematode patches, as it integrates tools such as: Global Navigation Satellite System (GNSS), Geographic Information Systems (GIS), Remote Sensing (RS), Wireless sensors (RSSF) and other techniques, equipment and software for obtaining useful information for agriculture (LÓPEZ *et al.*, 2015; LÓPEZ-RIQUELME *et al.*, 2017; ZHANG *et al.*, 2017). It enables decision making, ongoing crop monitoring, cost savings, increased productivity and intelligent control actions.

Precise detection and mapping of trouble spots in a field are products obtained using RS and GIS. The latter allow for better management practices, with localized treatment and within the timing of the crop. Several studies show the ability to detect the spatial distribution of a pathogen through thermography, spectroradiometers, multispectral and hyperspectral sensors on plant canopy spectral response (BAJWA *et al.*, 2017; JOALLAND *et al.*, 2017; MARTINELLI *et al.*, 2015; MARTINS *et al.*, 2017).

Orbital RS allows for a diagnosis of large areas in a short time and the determination of severity levels of nematode-infected plants (MARTINS *et al.*, 2017). With the miniaturization of sensor systems, drones allow timely mapping for detection of pathogens in large areas (YANG *et al.*, 2016), mapping of soil fertility responses (SCHUT *et al.*, 2018) and yield estimates (JEONG *et al.*, 2018).

For the infestation scenario present in our study areas, soybean health characterization maps obtained through unmanned aerial vehicles (UAVs), associated with directed sampling, can lead to fast and reliable methods for georeferenced detection of levels of nematode infestation. Thus, this study aimed to define the best spectral range for the detection of *H. glycines* and *P. brachyurus* by simple linear regressions in soybean crop at R3 stage, as well as the elaboration of mathematical models by multiple linear regressions.

MATERIAL AND METHODS

Study area characterization

The municipalities of Rio Verde and Montividiu, located in the State of Goiás and in places where their lands are valued for high fertility and high rainfall, have good topography conditions for grain management. However, the field located to the south of the state is marked by the presence of *H. glycines*, *P. brachyurus* and *Helicotylenchus dihystera* nematodes, as evidenced by the nematological analysis carried out by the Nematology Laboratory of the Federal Institute of Goiás (Figure 1).

Figure 1 - Location of the experimental area and the patches
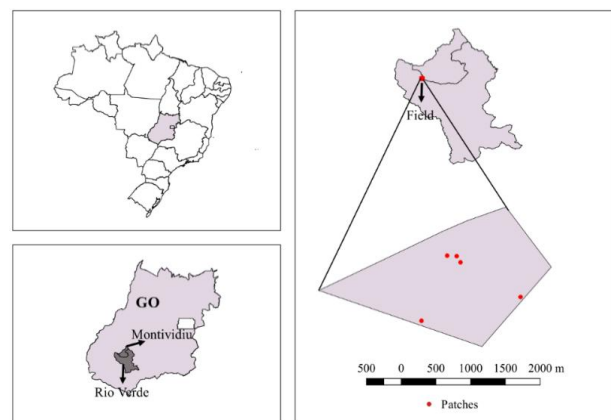
The experimental field was characterized by a topography with a slope of less than 5% to the southeast. No-till was predominant with the use of autopilot. The main location of the patches was in an old road that crossed the field, of which the last one has an area of approximately 330 hectares.

Material

A total of 45 sites were sampled to the elaboration of regressions and 60 sites for validation of two mathematical models: i. simple linear regression; and ii. multiple linear regression. An Unmanned Aerial Vehicle (UAV), known as Inspire 2, and a modified sensor with a total of 12 spectral bands were used to fly over the experimental area.

The camera aboard Inspire 2, known as Sentera, had 8 sensors, some of which were in the visible and others outside this spectral range. The device have the wavelength band of 615, 586, 661, 825 and 775 nanometers (nm), a composition sensor R (650 nm), G (548 nm), B (446 nm), a NDVI sensor containing one Red (625 nm) and one Nir (850 nm) band and a NDRE sensor containing another Nir band (840 nm) and one known as RedEdge (720 nm).

The 45 sampling sites, mapped by means of a georeferenced orthomosaic from the 2017/18 growing season, were identified in the field by a white sheet so that after the flight they could be precisely located. To reach the sites to be sampled, we used a Garmin eTrex 20 receiver. The *FieldAgent* application was used to perform the flight over the patches, the Pix4d software to obtain the orthomosaic and the Qgis software for extracting the information from the pixels of the sampled areas and mapping. Statistical analysis and data validation were performed in Minitab statistical software.

Nematode sampling

The soybean field used for soil and root sampling was planted on October 10, 2018 with the early cultivar MONSOY 7198, resistant to soybean cyst nematode races 1 and 3. The history of the area was known for the presence of *H. glycines* of races 1,3 and 6, *P. brachyurus* and *H. dihystera*.

A total of 105 nematode samples were collected, 45 for the regression calculation and 60 for the validation of mathematical models, with 3 subsamples for each site. The validation samples refer to an experimental area containing 60 plots. All samplings were obtained with a maximum of one day difference.

Figure 2 - Sites outside the plots of the experimental area comprise the samples used for the elaboration of linear regressions and sites inside the plots for the validation of regressions
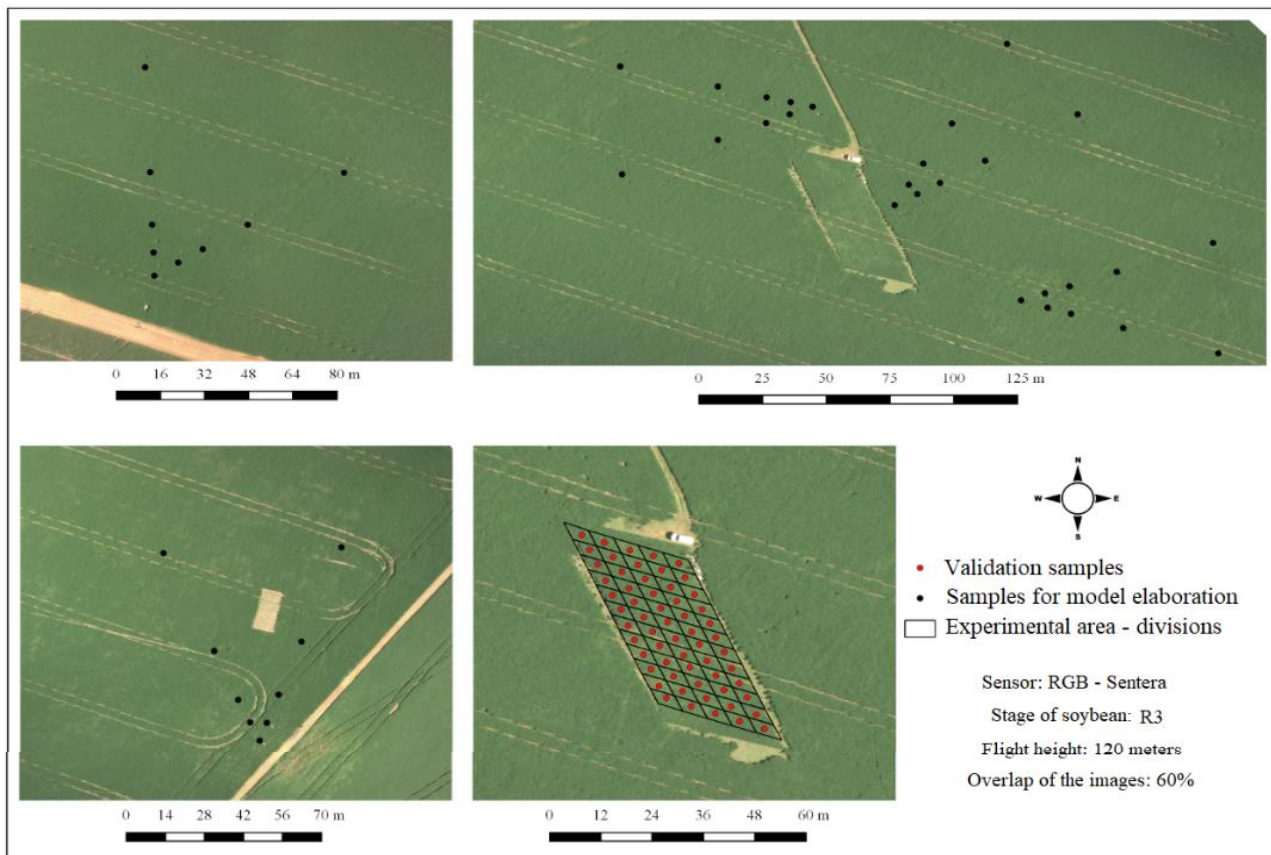
The samples for the elaboration of the single and multiple linear regression models were divided into 5 patches, so that one sampling site was at the center and the other in two different directions, 10, 20, 40 and 80 m from the center of the patch (Figure 2).

Samples were taken during the R3 stage of soybean at a depth of 0 to 20 cm. This stage was shrunk due to the reduction of soil interference with the value of the pixels used in the statistical analysis. For each site, besides the soil, the root of the cultivar was collected. Therefore, the samples were sent to the Phytopathology Laboratory of the Federal Institute of Goiás - Campus Rio Verde, for the extraction of juveniles, females and cysts and identification of nematodes. Races of *H. glycines* were identified in another laboratory, and they were forwarded by the farmer who allowed the research in his property.

The extraction of juvenile *P. brachyurus*, *H. dihystera* and *H. glycines* in soil and root were performed according to the methods of Jenkins (1964), Coolen and D'Herde (1972) and Alfenas and Mafia (2007). For viable and non-viable cysts in soil, we used the methodology adapted by Araújo (2009) and for females in root, the method adapted by Tihohod (2000).

Flight planning and orthomosaic construction

The flight was performed on the same sampling days, between 10:00 and 14:00, so that all sites were overflown. In the FieldAgent application, we set a 60% overlap between front and side of the images at a flight height of 120 meters, so that a battery was sufficient to fly over all the patches. Heterogeneous lighting conditions during photo capture were avoided as they alter the spectral response of plants and the results of statistical analysis, even with the use of the irradiance sensor.

Prior to the flight over the patches, some blank targets were placed at the sites to be sampled to facilitate identification in the image. It is important that the image information is extracted as close as possible to the soil and root collection, such that the spectral response refers to what is present at the site of the collected plant. For the experimental area, the plots were delimited by targets at their ends.

Orthomosaic was constructed by photogrammetric processing in the Pix4d software, with the provision of the camera's interior and exterior orientation parameters and the calculated point cloud. Therefore, no calibration panel was used for the reflectance calculation.

Image information extraction and prediction map construction

Through the orthomosaic, in each plant referring to the nematode data sampling sites, information on the amount of light reflected by the leaf canopy was extracted so that the value could be used in single and multiple linear regressions. The extraction for the 45 sites was performed in each of the 12 Sentera bands with the *feature identify* tool. The latter allows, with just one click on the image, the pixel value is expressed.

For each of the 45 samples of patches, the value of the light reflected by the canopy, used in the statistical analysis of single and multiple linear regressions, was the result of an average of 10 pixels extracted by the option *identify features*, without the presence of shade and soil.

As for obtaining the estimated value of non-viable cysts from the prediction map, we considered the pixel coincident with or overlapping the validation point located at the center of the plots. The prediction map of the single and multiple linear regression was generated using the *raster calculator*, with the mathematical equation of each of the two best regressions for non-viable cysts.

Statistical analysis and validation of two mathematical models

The correlations performed were between the nematode data and the pixel value of the images. Relationships between juveniles, cysts and females were analyzed with the amount of light reflected by the plant canopy for each of the sites and bands.

However, *H. dihystera* was not included in the statistical analysis because it is an ectoparasite that does not cause significant damage to soybean crop (ANTÔNIO, 1992). For simple linear regressions, only those significant at 5% were considered. The normality and independence test was applied to the residuals as well as the homogeneity of variance.

For multiple linear regressions, we used the forward stepwise methodology, which starts with a simple linear regression, and new variables are inserted into the model according to the adopted significance level (CHATTERJEE; HADI, 2015). It is only completed when the best mathematical model found is repeated again. A p-value of 0.05 was adopted in the model, uncorrelated independent variables and with the lowest possible Mallows Cp. Finally, normality tests and residual independence and homogeneity of variance were also performed.

For validation of the prediction model, from the measured and estimated data, the root-mean square error (RMSE) and the ERROR (%) were calculated. RMSE and ERROR (%) are obtained through equations 1 and 2.

$$RMSE = \sqrt{\sum_{i=1}^{n} (xi - xmed)^2 /_n} \tag{1}$$

$$ERROR(\%) = \sqrt{\sum_{i=1}^{n} (xi - xmed)^2 /_n} \, X \, \frac{100Xn}{\sum_{i=1}^{n} xmed} \tag{2}$$

where $\chi i \ldots and \cdots \chi - med$ represent the estimated and in situ measured value of non-viable cysts in 100 cm³ soil, respectively; and n is the number of samples.

RESULTS AND DISCUSSION

Of the three types of nematodes found in the patches, *P. brachyurus* and *H. dihystera* were the most abundant in the soil and root samples, and *H. glycines* of races 1, 3 and 6 were the least significant, due to the use of a cultivar resistant to races 1 and 3. To detect the presence of *H. glycines* in the experimental area, using simple linear regressions, the visible range showed good results of R² and p-value (Table 1).

Nevertheless, *P. brachyurus* cannot be detected by the sensor used here for soybean at R3 stage using a simple linear regression, as no result was significant at 5%. However, there is a spectral range of 586 nm that presented a p-value less than 0.001 and an R² of 0.6499, for non-viable cysts in soil. Although the cysts were in soil, they were hatched, indicating that symptoms caused at earlier stages by

the penetration of race 6 nematode into soybean roots contributed to a good detection at R3. Good results were also found in the Red and Green bands of the Sentera RGB sensor (Table 1), results similar to Bajwa *et al.* (2017), who also showed a high correlation from 500 nm to 700 nm for soybean cyst nematode.

Healthy soybean plants absorb more the Red, Green, in the range of 615 nm, 586 nm and 661 nm than plants affected by soybean cyst nematode. Thus, the greater the number of non-viable cysts, the greater the amount of light reflected by the plant in the bands mentioned above. This was also reported by Martins *et al.* (2017), for the case of the gall nematode in coffee crop. An increased reflection of red was also found by Bajwa *et al.* (2017) by the occurrence of cyst in soybean and by Santos Junior *et al.* (2002), which state that plants with lower cyst infection have a higher capacity for energy absorption of red.

Table 1- Simple linear regressions for the detection of *H. glycines*

Nematode variable	Range	Linear regression models		
		R²	p-value / F	Equation
Non-viable cyst	Red	0.6326	< 0.001 / 77.11	y = 1.7228 × Red -166.08
	Green	0.5888	< 0.001 / 61.57	y = 1.2185 × Green -153.67
	615 nm	0.1439	0.010 / 7.23	y = 0.7246 × 615 nm - 33.691
	586 nm	0.6499	< 0.001 / 79.82	y = 1.5813 × 586 nm -193.81
	661 nm	0.1346	0.013 / 6.69	y = 0.5859 × 661 nm -26.038
Viable cyst	Red	0.3481	< 0.001 / 23.02	y = 0.2104 × Red - 20.267
	Green	0.3198	< 0.001 / 20.22	y = 0.1488 × Green -18.754
	586 nm	0.3766	< 0.001 / 25.97	y = 0.1994 × 586 nm - 24.463
	Red - NDVI	0.0880	0.048 / 4.15	y = - 0.054 × Red (625 nm) + 4.0806

*gl of the residue (43)

Table 2 - Mathematical models for detection of *H. glycines* and *P. brachyurus*

Mathematical model for non-viable cyst	y = - 163.5 + 1.133 × Red + 0.697 × Green - 0.522 × 825 nm
R² (aj) / R² (pred)	0.7436 / 0.7213
p-value / F- Red	< 0.001 / 23.80
p-value / F - Green	< 0.001 / 16.31
p-value / F - 825 nm	0.014 / 6.53
Mallows Cp coefficient	6.8
Mathematical model for P. brachyurus in soil	y = - 458 +2.52 × Green + 2.52 × Nir (850 nm)
R² (aj) / R² (pred)	0.1368 / 0.00
p-value - Green	0.020 / 5.85
p-value – Nir - NDVI	0.049 / 4.09
Mallows Cp coefficient	8.5

*gl of the residue (Mathematical model for non-viable cyst) = 41, *gl of the residue (Mathematical model for non-viable cyst) = 42

In the case of viable cysts, the best detection band is the same as for non-viable cysts, but with an R² of 0.3766. Green and Red also stood out, with an R² of 0.3198 and 0.3481, respectively. However, cysts that have not yet hatched should not be taken into consideration for the detection of soybean cyst nematode, as they do not cause symptoms.

Table 2 presents a mathematical model elaborated using stepwise multiple linear regression, which presents better results than simple linear regressions for non-viable

Figure 3 - RGB composition of some sampled areas

cysts in soil. In addition, it also allows the detection of nematodes of root lesions present in soil, previously not observed by simple linear regression.

The prediction variables of the mathematical model for non-viable cysts consider two bands that showed good correlation results in simple linear regression, and one that is out of the visible range, which is 825 nm. None of the independent bands was correlated with each other, with the calculated VIF equal to 1 (TAMURA *et al*., 2019). Mallows Cp was 6.8, lower than other multiple linear regression models for non-viable cysts, which had an R² less than 0.7430. Thus, it was prioritizing Mallows Cp as close as possible to the number of predictors (MALLOWS, 2000).

In the case of *P. brachyurus*, although the multicollinearity of the model is adequate, the Mallows Cp of 8.5 indicates a low model precision and a high variance of regression coefficients. In Figure 3, there is the true-color composition of 3 patches, where samples were taken. The only patch of all studied, which was evident in the image, was the patch - 1, due to the larger amount of bare soil due to a smaller canopy size.

The subtle symptoms to human eyes present in the RGB composite image become more evident when a thematic map for predicting non-viable cysts is drawn through the 586 nm band for simple linear
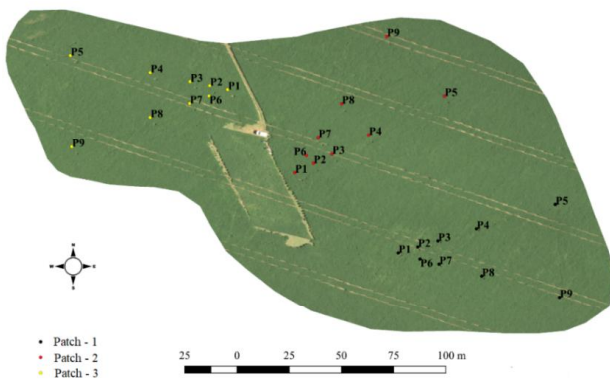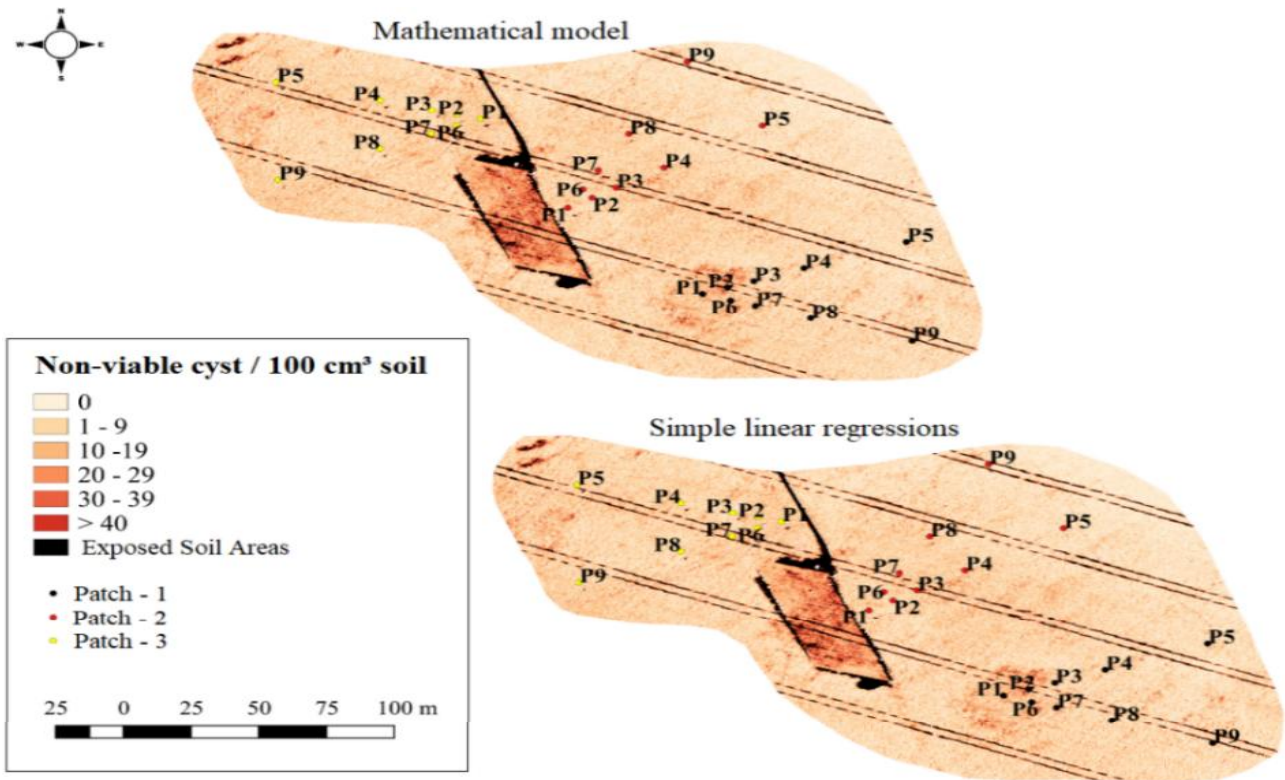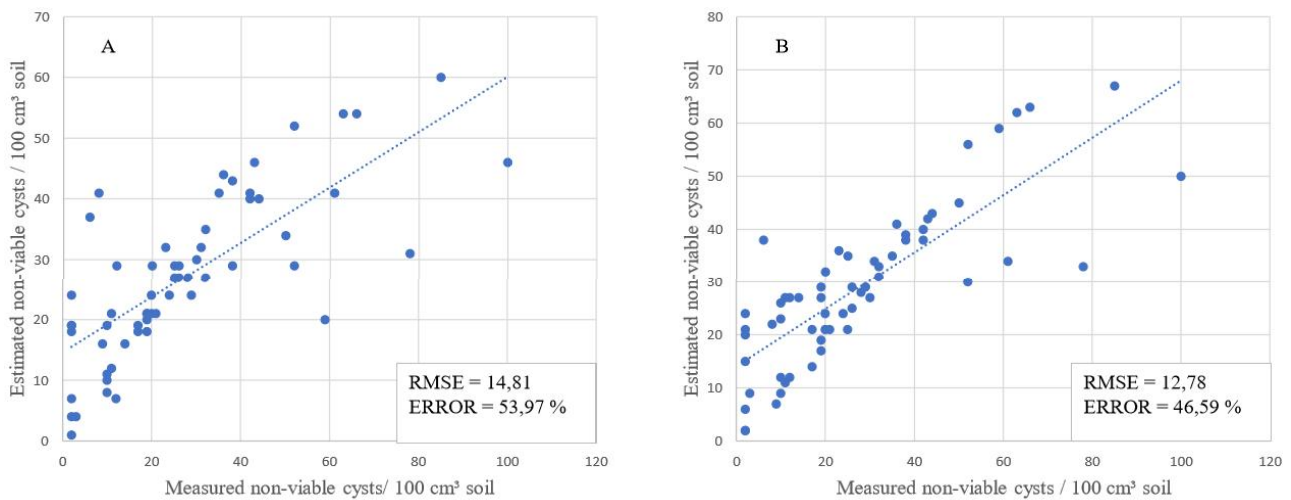
Figure 4 - Prediction map made using simple linear regression and prediction map made using multiple linear regression

Figure 5 - A- RMSE and ERROR of simple linear regression with 586 nm band for detection of non-viable cysts; B - RMSE and ERROR of the mathematical model for detection of non-viable cysts

regression, and through multiple linear regression, which presented an R^2 of 0.7430 (Figure 4).

Figure 5 presents the performance of the prediction model expressed by the root mean square error (RMSE). They have similar but distinct results. The model using simple linear regression presented an RMSE of 14.81, with an error of 53.97%. In turn, the mathematical model, somewhat better, presented an RMSE of 12.78 and an error of 46.59% (Figure 5). Such values are satisfactory, considering that the nematode population can vary greatly from site to site within a few tenths of a centimeter. They all had a p-value less than 0.05.

Although prediction maps have a high error, they can be used for preliminary detection of sites with higher and lower occurrence of *H. glycines*, so that soil sampling can be directed and quantification improved. This is valid as the areas to be monitored are extensive and the soil sampling is expensive and time consuming (MARTINS *et al.*, 2017). In summary, with some soil samples and the georeferenced thematic map, it is possible to reduce the costs of nematicide application (ALJAAFRI, 2017), which makes control sustainable and viable, with intelligent application.

CONCLUSIONS

1. For detection of *H. glycines,* the best spectral range was 586 nm, which presented an R^2 of 0.649 for non-viable cysts in soil. In simple linear regression, nothing was significant for the detection of *P. brachyurus*;

2. However, when the Green and Nir-NDVI bands are combined in a mathematical model, *P. brachyurus* in soil becomes significant and detected. In the case of the mathematical model for detection of *H. glycines*, specifically the non-viable cysts, a significant improvement in R^2 is achieved, combining the Red, Green and 825 nm bands;

3. By validating the two mathematical models, both for detection of non-viable cysts in soil, it was possible to prove the efficiency in the detection of sites with larger and smaller amounts of nematodes. This is important so that the number of soil samples can be reduced and targeted so as to produce a good application map at a variable rate. The best prediction result was the one that used multiple linear regression.

REFERENCES

ALFENAS, A. C.; MAFIA, R. G. **Métodos em fitopatologia**. 2. ed. Viçosa, MG: Universidade Federal de Viçosa, 2007. 516 p.

ALJAAFRI, W. A. R. **Management of plant-parasitic nematodes using gene manipulation and biological nematicides**. Mississippi: Mississippi State University, 2017. 176 p.

ANTÔNIO, H. Fitonematóides na cultura da soja. **Informe Agropecuário**, v. 16, n. 172, p. 60-65, 1992.

ARAÚJO, F. G. D. **Quantificação de machos e fêmeas de *Heterodera glycines* (*Ichinohe*, 1952) em cultivares de soja resistentes e suscetíveis**. 2009. 38 p. Dissertação (Mestrado em Ciências Agrárias) – Universidade Federal de Goiás, Goiânia, 2009.

BAJWA, S. G. *et al.* Soybean disease monitoring with leaf reflectance. **Remote Sensing**, v. 9, n. 2, p. 127, 2017. DOI: 10.3390/rs9020127.

CHATTERJEE, S.; HADI, A. S. **Regression analysis by example**. 2. ed. New York: Wiley, 2015. 389 p.

COOLEN, W. A.; D'HERDE, C. J. **A method for the quantitative extraction of nematodes from plant tissue**. Ghent: State Nematology and Entomology Research Station, 1972. 77 p.

DUTTA, T. K. *et al*. Plant-parasitic nematode management via biofumigation using brassica and non-brassica plants: current status and future prospects. **Current Plant Biology**, v. 17, p. 17-32, 2019. DOI: 10.1016/j.cpb.2019.02.001.

HOMIAK, J. A. *et al*. Seed treatments associated with resistance inducers for management of *Pratylenchus brachyurus* in soybean. **Phytoparasitica**, v. 45, n. 2, p. 243-250, 2017. DOI: 10.1007/s12600-017-0575-0.

JENKINS, W. R. B. *et al*. A rapid centrifugal-flotation technique for separating nematodes from soil. **Plant Disease Reporter**, v. 48, n. 9, 1964.

JEONG, S. *et al*. Application of an unmanned aerial system for monitoring paddy productivity using the GRAMI-rice model. **International Journal of Remote Sensing**, v. 39, n. 8, p. 2441-2462, 2018. DOI: 10.1080/01431161.2018.1425567.

JOALLAND, S. *et al.* Comparison of visible imaging, thermography and spectrometry methods to evaluate the effect of *Heterodera schachtii* inoculation on sugar beets. **Plant Methods**, v. 13, n. 1, p. 73, 2017. DOI: 10.1186/s13007-017-0223-1.

LÓPEZ, J. A. *et al*. A multifunctional wireless device for enhancing crop management. **Agricultural Water Management**, v. 151, p. 75-86, 2015. DOI: 10.1016/j.agwat.2014.10.023.

LÓPEZ-RIQUELME, J. *et al*. A software architecture based on FIWARE cloud for Precision Agriculture. **Agricultural Water Management**, v. 183, p. 123-135, 2017. DOI: 10.1016/j.agwat.2016.10.020.

MALLOWS, C. L. Some comments on Cp. **Technometrics**, v. 42, n. 1, p. 87-94, 2000. DOI: 10.1080/00401706.2000.10485984.

MARTINELLI, F. *et al*. Advanced methods of plant disease detection: a review. **Agronomy for Sustainable Development**, v. 35, n. 1, p. 1-25, 2015. DOI: 10.1007/s13593-014-0246-1.

MARTINS, G. D. *et al.* Detecting and mapping root-knot nematode infection in coffee crop using remote sensing measurements. **IEEE Journal of Selected Topics in Applied Earth Observations and Remote Sensing**, v. 10, n. 12, p. 5395-5403, 2017. DOI: 10.1109/JSTARS.2017.2737618.

MASONBRINK, R. *et al*. The genome of the soybean cyst nematode (*Heterodera glycines*) reveals complex patterns of duplications involved in the evolution of parasitism genes. **BMC Genomics**, v. 20, n. 1, p. 1-14, 2019. DOI: 10.1186/s12864-019-5485-8.

NIBLACK, T. L. Soybean cyst nematode management reconsidered. **Plant Disease**, v. 89, n. 10, p. 1020-1026, 2005. DOI: 10.1094/PD-89-1020.

SANTANA-GOMES, S. D. M. *et al*. Sucessão de culturas no manejo de *Pratylenchus brachyurus* em soja. **Nematropica**, v. 44, n. 2, p. 200-206, 2014.

SANTOS JUNIOR, R. F. dos. *et al*. Detection of infested areas with Heterodera glycines in a soybean field using spectroradiometry in the visible and near infrared. **Fitopatologia Brasileira**, v. 27, n. 4, p. 355-360, 2002.

SCHUT, A. G. *et al*. Assessing yield and fertilizer response in heterogeneous smallholder fields with UAVs and satellites. **Field Crops Research**, v. 221, p. 98-107, 2018. DOI: 10.1016/j.fcr.2018.02.018.

SONG, J. *et al*. Assessment of parasitic fungi for reducing soybean cyst nematode with suppressive soil in soybean fields of northeast China. **Acta Agriculturae Scandinavica, Section B—Soil & Plant Science**, v. 67, n. 8, p. 730-736, 2017. DOI: 10.1080/09064710.2017.1343377.

TAMURA, R. *et al*. Mixed integer quadratic optimization formulations for eliminating multicollinearity based on variance inflation factor. **Journal of Global Optimization**, v. 73, n. 2, p. 431-446, 2019. DOI: 10.1007/s10898-018-0713-3.

TIHOHOD, D. **Nematologia agrícola aplicada**. 2. ed. Jaboticabal: Funep, 2000. 372 p.

UNITED STATES DEPARTMENT OF AGRICULTURE. **Oilseeds**: world markets and trade. Disponível em: https://apps.fas.usda.gov/psdonline/circulars. Acesso em: 12 abr. 2019.

YANG, C. *et al*. Change detection of cotton root rot infection over 10-year intervals using airborne multispectral imagery. **Computers and Electronics in Agriculture**, v. 123, p. 154-162, 2016. DOI: 10.1016/j.compag.2016.02.026.

ZHANG, H. *et al*. Genetic architecture of wild soybean (*Glycine soja*) response to soybean cyst nematode (*Heterodera glycines*). **Molecular Genetics and Genomics**, v. 292, n. 6, p. 1257-1265, 2017. DOI: 10.1007/s00438-017-1345-x.